JOURNAL OF THEORETICAL
AND APPLIED MECHANICS
https://doi.org/10.15632/jtam-pl/210426
ONLINE FIRST

RESEARCH ON THE ENERGY RECOVERY SYSTEM IN THE ACTIVE HORIZONTAL SEAT SUSPENSION OF A WORKING MACHINE

Bartosz JERECZEK*, Igor MACIEJEWSKI, Andrzej BŁAŻEJEWSKI,
Sebastian PECOLT, Tomasz KRZYŻYŃSKI

Faculty of Mechanical and Energy Engineering, Koszalin University of Technology, Koszalin, Poland
*corresponding author, *bartosz.jereczek@tu.koszalin.pl*

This paper investigates the potential for longitudinal vibration energy recovery in a seat suspension system through the implementation of a brushless direct current (BLDC) motor. The work focuses on two states of system operation. The first one is when an electric motor works as an actuator in the powering mode to withstand horizontal forces. The second one occurs in the regenerative mode when the kinetic energy of the system is partially converted into electricity. Within the scope of the presented study, the efficiency of the energy regeneration process under random vibration conditions of different intensities is investigated experimentally. Measurement results are presented in the form of vibration transmittance functions for a suspension with energy regeneration compared to a conventional passive and fully active system.

Keywords: vibrations; seat suspension; active system; energy harvesting; recuperative braking.

1. Introduction

One of the main areas of current studies in mechanical and electrical engineering is energy harvesting from vibrating systems. The process by which mechanical energy produced by system or ambient vibrations is transformed into useable electrical energy is the basis for the phenomenon. It can be utilized to lower the system's overall energy consumption or to power (Paul *et al.*, 2021) self-sufficient technology, like IoT in case sensors (Shrestha *et al.*, 2022; Rehman *et al.*, 2024). Electrostatic, piezoelectric and electromagnetic solutions are the main techniques for recovering energy from vibrations. Their characteristics vary, affecting their range of applications, implementation constraints and efficiency. Both active (Hoić *et al.*, 2024) and semi-active (Wei & Pang, 2023) seat suspension systems can take advantage of recuperative braking. As stated in (Sun *et al.*, 2018), the PMSM motor, serving as an electromagnetic damper, is mounted to the vehicle body and the unsprung mass. By connecting motor phases in different series-parallel resistor configurations, this solution offers semi-active control of the seat suspension system and enables the control of the suspension damping force through an external circuit with resistors and MOSFET drivers.

This paper expands on the concept of utilizing a brushless direct current (BLDC) motor as a force generator to counteract seat suspension forces or as an energy harvester in the regenerative braking mode. In summary, harnessing supplementary energy from operational devices

Ministry of Science and Higher Education
Republic of Poland

This publication has been funded by the Polish Ministry of Science and Higher Education under the Excellent Science II programme "Support for scientific conferences".
The content of this article was presented during the 61st Symposium "Modelowanie w mechanice" (Modelling in Mechanics), Szczyrk, Poland, March 2–5, 2025.

is a superior alternative to utilizing conventional batteries as a power source for equipment, as it yields a lower overall energy value delivered to the system, thereby enhancing the energy utilization coefficient and reducing operational costs.

2. Model of horizontal seat suspension and hardware implementation

Figure 1a illustrates a physical representation of a horizontal seat suspension system featuring an active control mode and an energy harvesting device. The passive system comprises two tension springs operating in opposing directions, facilitating the establishment of a static equilibrium position for a seat suspension burdened by the suspended mass. A hydraulic damper is utilized to diminish the amplitude of resonant vibrations in the passive system. This system operates effectively under low-friction conditions, facilitated by needle bearings in the suspension mechanism. Additionally, the seat suspension is equipped with end-stop buffers that restrict movement to a maximum displacement of the suspension system. The active system comprises an induction motor for active vibration control (active motoring mode) and for energy harvesting (regenerative braking mode). Figure 1b illustrates the actual experimental apparatus employed to evaluate the vibro-isolation characteristics of the seat. The seat is affixed to a test rig equipped with mechanical components that replicate actual vibrations and forces. Dimensions of the suspension mechanism are as follows: length 425 mm, width 255 mm, height 225 mm. Its unsprung mass, in turn, is about 8 kg and the sprung mass is approximately 7 kg. The configuration comprises sensors and actuators to assess the reaction of the seat to vibrations, guaranteeing that the active suspension system can efficiently lessen undesirable oscillations.

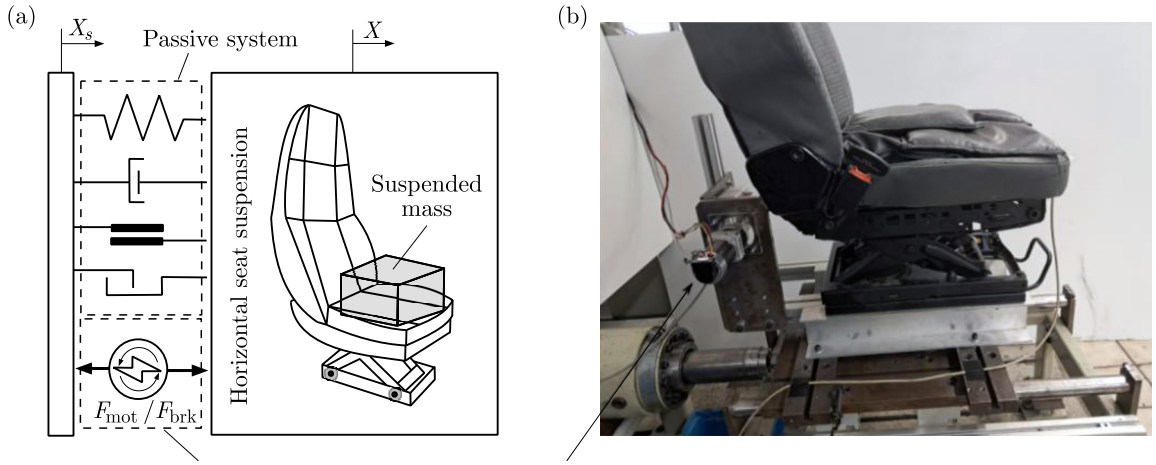

Fig. 1. Physical model of horizontal seat suspension system with active motoring and regenerative braking (a) and set-up for experimental investigation of the vibro-isolation effectiveness (b).

Energy harvesting occurs solely when the intended active force F_{mot} exhibits a sign contrary to the relative velocity $\dot{x} - \dot{x}_s$ of the suspension system (where $\dot{x}$ represents the velocity of seat and $\dot{x}_s$ denotes the velocity of input vibration). In the opposite situation, the vibration reduction system operates by drawing electricity from an external energy source. To generate an active force, a brushless three-phase electric motor cooperates with the system for harvesting energy from mechanical vibrations (Fig. 2). The motor operation is controlled by a dedicated controller that regulates parameters based on input signals, such as torque and rotation direction. The analogue regenerative braking signal, originating from the system controller, is converted into a digital form by a microcontroller. Then, one of five signals generated in this process (ST_1, ST_2, ST_3, ST_4, ST_5) is used to control one of the braking resistor groups (R_1, R_2, R_3, R_4, R_5) via MOSFET transistors.

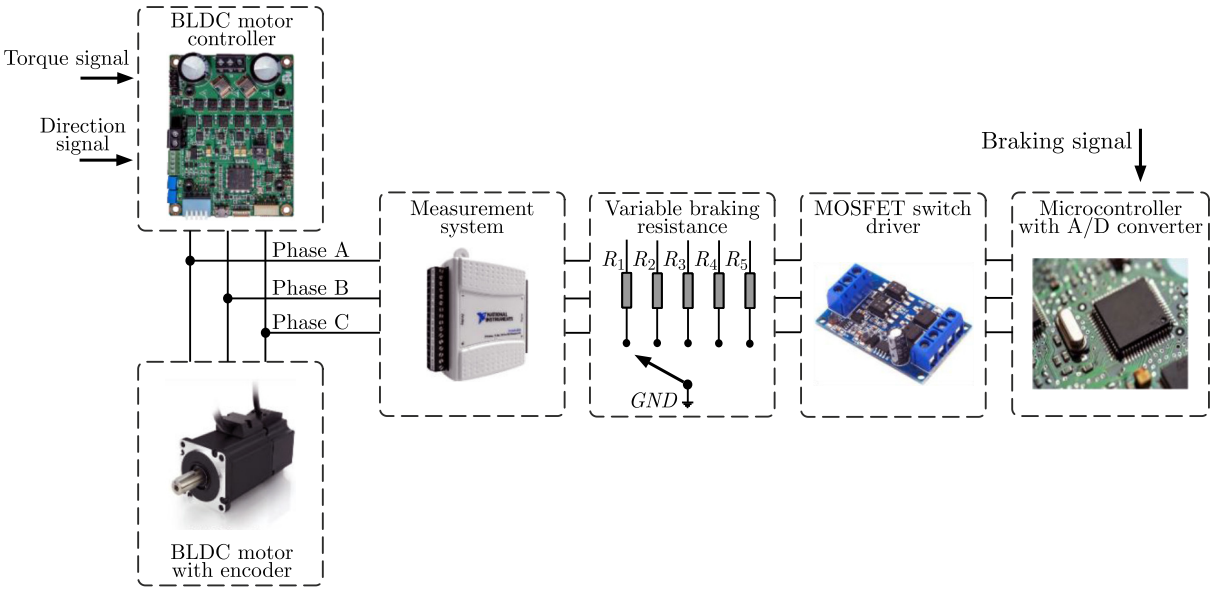

Fig. 2. Hardware implementation of the energy recovery braking subsystem.

The intensity of regenerative braking is regulated through the binary selection of one of five braking resistor groups with resistances of: 0.1 Ω for R_1, 0.15 Ω for R_2, 0.22 Ω for R_3, 0.33 Ω for R_4, and 0.47 Ω for R_5 that was determined experimentally to obtain proportionally varying braking force values (lower resistance is equal to higher braking force). Resistor groups are connected to the phases of the BLDC motor. At any given moment, only one resistor group is activated, allowing control over braking force and achieving various levels of energy recovery. The selection process provides straightforward regulations, although it may limit the smooth adjustment of braking force in real-time. The switching time between resistor groups is a key factor influencing system efficiency, as it determines the responsiveness to changes in the regenerative braking signal. The induced currents and voltages on the BLDC motor braking resistors are recorded by the data acquisition system, enabling their analysis and potential optimization of the energy recovery process.

3. Experimental research

Figure 3 shows white noise excitation signals, which were used to excite the dynamic response of the tested system. Figure 3a presents the time course of the displacement. All three signals exhibit a similar random character, but there are slight differences in amplitude. The waveforms are characterized by maximum deflections in the range of ±0.025 m. Figure 3b shows spectra of the same signals in the frequency domain. Their energy is distributed across a frequency band up to 10 Hz. The differences in power spectral density (PSD) levels indicate variable excitation intensity in individual samples. The research detailed in the paper was conducted using these

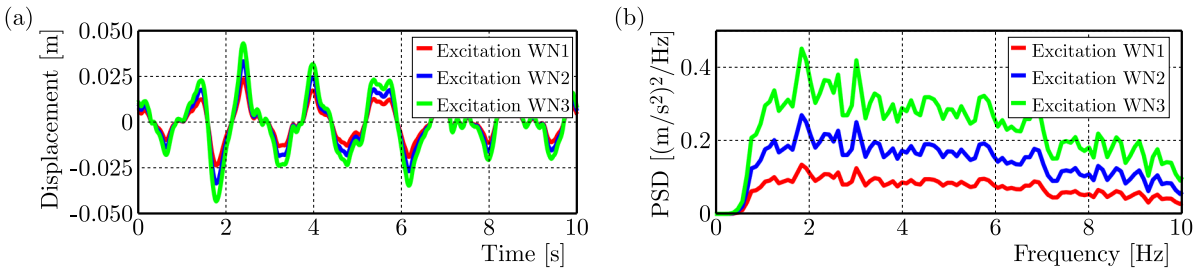

Fig. 3. Displacement of the random input vibration (a) and the PSD of acceleration signal (b) at different excitation intensities (WN1–WN3).

signals, and each test was carried out for a duration of three minutes. The tests are performed by using the mass load up to 80 kg. It directly loads the seat (reproducing upper part of the human body) that reflects the mass of a person weighing approximately 105 kg since the operator supports himself with his limbs.

Figure 4 presents the transmissibility functions of passive (Figs. 4a, 4b), active (Figs. 4c, 4d), and regenerative (Figs. 4e, 4f) seat suspension systems under different excitation intensities (WN1–WN3) and mass loads (40 kg and 80 kg). The transmissibility is plotted against the frequency (0 Hz–10 Hz), which is the key range for ride comfort analysis. The passive seat suspension system in Fig. 4a (WN1 (40 kg) versus WN3 (80 kg)) shows that at low excitation intensity (WN1) with a smaller load (40 kg), the transmissibility is slightly lower at resonance approx. 1 Hz–2 Hz, the red line, compared to the heavier load (80 kg) and higher excitation intensity (WN3), the blue line. Both curves exhibit a clear resonance peak around 1 Hz–2 Hz, typical of passive systems. Transmissibility decreases beyond the resonance frequency in both cases, but faster in the case of WN3 (80 kg). Figure 4b shows the case WN1 (80 kg) versus WN3 (40 kg). The clear peak transmissibility is higher for the smaller load (40 kg) with a higher excitation (WN3), the blue line, than for the heavier load (80 kg) with a lower excitation (WN1), the red line. This is characteristic for very low frequencies (below 1 Hz). Behind this range both curves exhibit a clear resonance peak around 1 Hz–2 Hz, with a slight shift (towards 2 Hz) of the maximum value for the WN3 (40 kg) configuration. This indicates sensitivity of passive systems to mass and excitation changes.

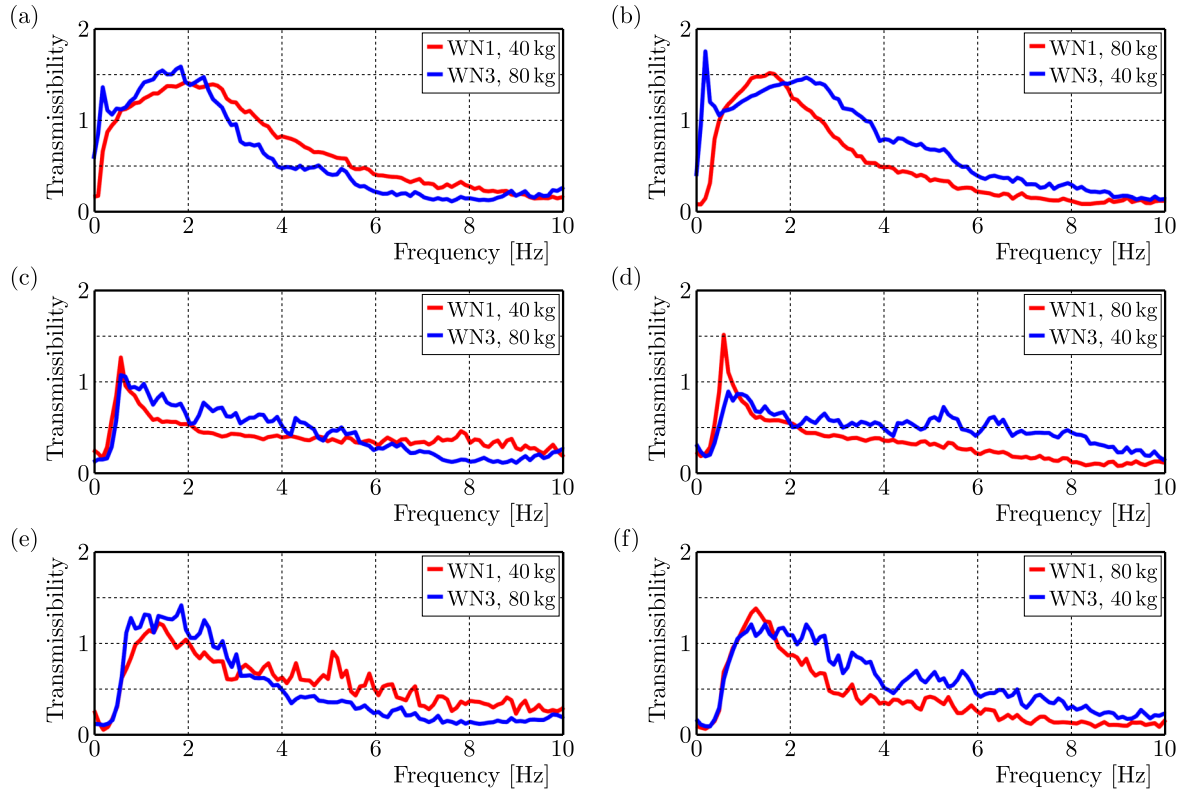

Fig. 4. Transmissibility functions of the passive (a)-(b), active (c)-(d), and regenerative (e)-(f) seat suspension system at different excitation intensity: WN1–WN3, and at various mass loads: 40 kg–80 kg.

In Fig. 4c the active seat suspension system response is presented, where two configurations WN1 (40 kg) versus WN3 (80 kg) are compared. The resonance peak is notably reduced compared to passive systems, showing active damping effectiveness. Overall lower transmissibility, especially at 1 Hz–3 Hz, is observed. The system performs better at lower excitation and lighter mass (red line) but still controls vibration effectively at higher intensity and mass. For the

configuration WN3 (80 kg), the active system seems to perform better above 6 Hz. Figure 4d (WN1 (80 kg) versus WN3 (40 kg)) shows a similar trend, i.e., active control reduces transmissibility across frequencies. The clear peak far above the transmissibility value of 1 occurs for the configuration WN1 (80 kg). Slight variations in performance depend on load and excitation, but overall stability is maintained. The regenerative seat suspension system is shown in Fig. 4e for configurations WN1 (40 kg) versus WN3 (80 kg). It is comparable to the active system in terms of reduced resonance peaks. It maintains lower transmissibility at mid and high frequencies (3 Hz–10 Hz) and shows good performance even at higher mass and excitation. In Fig. 4f (WN1 (80 kg) versus WN3 (40 kg)), resonance damping is slightly less effective than the purely active system but better than the passive one. This shows balance between damping and energy recovery without significant compromise in comfort.

The values in Table 1 provide numerical insights into the regenerative performance (in terms of RMS current and power) of a regenerative seat suspension system under varied excitation intensities (WN1–WN3) and mass loads (40 kg–80 kg). These results correlate directly with the transmissibility trends shown in Figs. 4e, 4f, offering a combined perspective on both ride comfort and energy harvesting potential.

Table 1. Numerical values of the regenerated RMS current and RMS power at different excitation intensity: WN1–WN3, and at various mass loads: 40 kg–80 kg.

Input vibration	Mass load					
	40 kg		60 kg		80 kg	
	RMS current	RMS power	RMS current	RMS power	RMS current	RMS power
WN1	1.020 A	2.130 W	1.152 A	2.428 W	1.195 A	2.613 W
WN2	1.714 A	4.229 W	1.849 A	4.584 W	2.061 A	5.735 W
WN3	2.338 A	6.401 W	2.502 A	7.009 W	2.654 A	7.692 W

In Table 1, the proportional effect of excitation intensity (from WN1 to WN3) is seen in that both RMS current and power increase monotonically with higher excitation, across all mass loads. This is expected as higher excitation introduces more energy, allowing the regenerative system to harvest more. The effect of the mass load (from 40 kg to 80 kg) is noticed as well because RMS current and power increase with heavier loads for each excitation level.

4. Conclusions

This research clearly demonstrates that active and regenerative suspension systems outperform passive systems in maintaining lower transmissibility across frequencies and under different mass and excitation conditions. Overall, heavier mass increases inertial forces, causing greater relative motion in the suspension system and leading to higher energy recovery. The increase is nonlinear but consistent, suggesting the system scales well with input energy and mass. Even under high excitation, the regenerative system maintains low transmissibility, indicating again the balance between comfort and power generation. Subsequent efforts will concentrate on enhancing the ratio of recovered energy to energy consumed during operation. This will be accomplished by enhancing the control algorithm and optimizing the electrical system that manages the transition between power and braking states.

References

1. Hoić, M., Kranjčević, N., & Birt, D. (2024). Design of an active seat suspension based on the Kempe mechanism. *2024 21st International Conference on Mechatronics – Mechatronika (ME)*, 1–7. https://doi.org/10.1109/ME61309.2024.10789764

2. Paul, K., Amann, A., & Roy, S. (2021). Tapered nonlinear vibration energy harvester for powering Internet of Things. *Applied Energy*, *283*, Article 116267. https://doi.org/10.1016/j.apenergy.2020.116267

3. Rehman, S.U., Usman, M., Toor, M.H.Y., & Hussaini, Q.A. (2024). Advancing structural health monitoring: A vibration-based IoT approach for remote real-time systems. *Sensors and Actuators A: Physical*, *365*, Article 114863. https://doi.org/10.1016/j.sna.2023.114863

4. Shrestha, K., Sharma, S., Pradhan, G.B., Bhatta, T., Rana, S.S., Lee, S., Seonu, S., Shin, Y., & Park, J.Y. (2022). A triboelectric driven rectification free self-charging supercapacitor for smart IoT applications. *Nano Energy*, *102*, 107713. https://doi.org/10.1016/j.nanoen.2022.107713

5. Sun, S., Dai, X., Wang, K., Xiang, X., Ding, G., & Zhao, X. (2018). Nonlinear electromagnetic vibration energy harvester with closed magnetic circuit. *IEEE Magnetics Letters*, *9*, 1–4, Article 6102604. https://doi.org/10.1109/LMAG.2018.2822625

6. Wei, C., & Pang, X. (2023). Modeling and simulation for a novel semi-active seat-suspension with a cam-roller-spring mechanism. *2023 6th International Conference on Intelligent Robotics and Control Engineering (IRCE)*, 108–112. https://doi.org/10.1109/IRCE59430.2023.10254784

Manuscript received June 16, 2025; accepted for publication September 8, 2025; published online September 20, 2025.